

Radiative QCD backgrounds to exclusive $H \rightarrow b\bar{b}$ production: radiation from the screening gluon

V.A. KHOZE^{a,b}, M.G. RYSKIN^{a,b} AND A.D.MARTIN^a

^a Department of Physics and Institute for Particle Physics Phenomenology,
University of Durham, DH1 3LE, UK

^b Petersburg Nuclear Physics Institute, Gatchina, St. Petersburg, 188300, Russia

Abstract

Central exclusive Higgs boson production, $pp \rightarrow p \oplus H \oplus p$, at the LHC can provide an important complementary contribution to the comprehensive study of the Higgs sector in a remarkably clean topology. The $b\bar{b}$ Higgs decay mode is especially attractive, and for certain BSM scenarios may even become *the* discovery channel. Obvious requirements for the success of such exclusive measurements are strongly suppressed and controllable backgrounds. One potential source of background comes from additional gluon radiation which leads to a three-jet $b\bar{b}g$ final state. We perform an explicit calculation of the subprocesses $gg \rightarrow q\bar{q}g$, $gg \rightarrow ggg$ in the case of ‘internal’ gluon radiation from the spectator, t -channel screening gluon, when the two incoming active t -channel gluons form a colour octet. We find that the overall contribution of this source of background is orders of magnitude lower than that caused by the main irreducible background resulting from the $gg^{PP} \rightarrow b\bar{b}$ subprocess. Therefore, this background contribution can be safely neglected.

1 Introduction

The search for the Higgs boson(s) is one of the main goals of the ATLAS and CMS experiments at the LHC. Once the Higgs boson is discovered, it will be of primary importance to determine its spin and parity, and to measure precisely the mass, width and couplings. A comprehensive study of the whole Higgs sector, including precision mass and coupling measurements, spin and CP properties, will be the next stage. Measurements of various important properties of the Higgs sector may be very challenging for the traditional LHC searches. In particular, the direct determination of the $b\bar{b}$ Yukawa coupling is inaccessible due to overwhelming QCD backgrounds. Moreover, nearly degenerate Higgs-like states are extremely difficult to separate. The spin-parity identification in many popular ‘Beyond the Standard Model’ (BSM) scenarios, as well as an observation of possible ‘invisible’ Higgs decays, exemplify other challenging issues.

The conventional strategy to achieve the ambitious programme of a complete study of the properties of the Higgs sector requires an intensive interplay between the LHC and the ILC (high-energy linear e^+e^- collider), see for example, [1]. Whilst awaiting the possible arrival of the ILC, there has been a growing interest in recent years in the possibility to complement the standard LHC physics menu by installing near-beam proton detectors in the LHC tunnel some 420 m from the ATLAS and CMS interaction points [2, 3]. In this way we may address many of the challenging issues well before the ILC has become operational, see, for example, [4] - [13] and references therein.

Although experimentally difficult, the forward proton mode at the LHC would provide an exceptionally clean environment to search for, and to identify the nature of, new objects, in particular, Higgs-like bosons. The expected cross sections are very small (about four orders of magnitude lower than those for the standard inclusive processes). Thus, an obvious requirement for the success of such measurements is that the backgrounds should be strongly suppressed and controllable.

Recall that, though the expected total production cross section for the SM Higgs at the LHC is rather large (around 50 pb), in order to identify the signal in the quite hostile background environment we have to rely, either on rare decay modes such as $H \rightarrow \gamma\gamma$, or to impose very severe cuts on the final state configurations¹. This unavoidably leads to a strong reduction (typically, by 3-4 orders of magnitude) of the observed cross sections. In this work we revisit the evaluation of the QCD backgrounds to exclusive $H \rightarrow b\bar{b}$ production at the LHC. Previous studies can be found in [5, 6], [14] - [17]. However, the main emphasis here is on radiation off the so-called screening gluon in the basic QCD diagram for exclusive $b\bar{b}$ production. This has not been quantified before.

The structure of the paper is as follows. In Section 2 we recall the formalism used to calculate the cross section of central exclusive Higgs boson production. Then in Section 3 the main sources of background to the $pp \rightarrow p + (H \rightarrow b\bar{b}) + p$ signal are considered. In Section 4 we describe the structure of the amplitude of internal gluon radiation from the screening gluon, while in Sections 5 and 6, respectively, the cross sections for the hard subprocesses of $b\bar{b}$ and gg dijet production in a colour-octet state are calculated. The numerical results are presented

¹ In this respect a selection of the quasi-three body pHp final state could be viewed as an extreme example of a final state cut.

in Section 7, and a brief summary given in Section 8.

2 Central Exclusive Diffractive Higgs Production

The central exclusive production (CEP) of a Higgs boson is the process $pp \rightarrow p \oplus H \oplus p$, where the \oplus denote the presence of large rapidity gaps between the outgoing protons and the decay products of the central system. As already mentioned, CEP offers a unique complementary measurement to the conventional Higgs search channels. First, if the outgoing protons scatter through small angles, then, to a very good approximation, the primary active di-gluon system obeys a $J_z = 0$, CP -even selection rule [18]. Here J_z is the projection of the total angular momentum along the proton beam axis. The observation of the Higgs boson in the CEP channel, therefore, determines the Higgs quantum numbers to be dominantly $J^{PC} = 0^{++}$, see [9, 19] for details. Secondly, because the process is exclusive, all of the energy/momentum lost by the protons during the interaction goes into the production of the central system. Measuring the outgoing protons allows the central mass, M_H , to be determined with an accuracy of just a few GeV regardless of the decay products of the central system. At the same time, the equality of the accurate missing-mass reconstruction of the Higgs, M_H , with its mass determined in the central detector from the decay products allows the background to be considerably suppressed. A precision missing-mass measurement requires dedicated forward proton detectors to be installed in the high dispersion region 420 m either side of the ATLAS and/or CMS interaction points². It is important to note that a signal-to-background ratio of order 1 (or even better) is achievable [18, 5]. As discussed in [6, 7], CEP processes would enable a unique signature for the MSSM Higgs sector, in particular allowing the direct measurement of the Hbb Yukawa coupling. Furthermore, CEP can provide valuable information on the Higgs sector of NMSSM [11] and other popular BSM scenarios, and can, for example, be also beneficial in searches for Higgs triplets [13].

Finally, in some BSM schemes this mechanism provides an opportunity for lineshape analysis [10, 9], including the Higgs width measurement in the case of large width, and allows the direct observation of a CP -violating signal [10, 20]. As already mentioned, the final-state structure is much cleaner than in the (messy) non-diffractive environment, and the event kinematics are strongly constrained by measuring the outgoing protons. Moreover, the study of the azimuthal correlations between the final protons would allow a straightforward approach to probe the CP structure of the Higgs sector [20].

The theoretical formalism [21] - [26] for central exclusive production contains distinct parts, as illustrated in Fig. 1. The cross section can be written schematically in the form [4, 21]

$$\sigma(pp \rightarrow p + H + p) \sim \frac{\langle S^2 \rangle}{B^2} \left| N \int \frac{dQ_t^2}{Q_t^4} f_g(x_1, x'_1, Q_t^2, \mu^2) f_g(x_2, x'_2, Q_t^2, \mu^2) \right|^2 \quad (1)$$

where $B/2$ is the t -slope of the proton-Pomeron vertex, $\langle S^2 \rangle$ is the so-called survival probability of the rapidity gaps, and the normalization, N , is given in terms of the $H \rightarrow gg$ decay width. The amplitude-squared factor, $|\dots|^2$, can be calculated in perturbative QCD because

²We refer the reader to the FP420 R&D report for experimental and detector details [2].

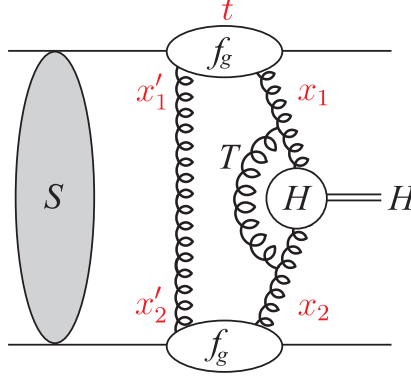


Figure 1: A symbolic diagram for the central exclusive production of a Higgs boson H .

the dominant contribution to the integral comes from the region $\Lambda_{\text{QCD}}^2 \ll Q_t^2 \ll M_H^2$ for the large Higgs mass values of interest [21]. The probability amplitudes, f_g , to find the appropriate pairs of t -channel gluons (x_1, x'_1) and (x_2, x'_2) are given by skewed unintegrated gluon densities at a hard scale $\mu \sim M_H/2$. These generalized gluon distributions are usually taken at $p_t = 0$, and then the “total” exclusive cross section is calculated by integrating over the transverse momentum, p_T , of the recoil protons. If we assume an exponential behaviour then, using

$$\int dp_T^2 e^{-B p_T^2} = 1/B = \langle p_T^2 \rangle, \quad (2)$$

we see that the additional factor in (1) is $\langle S^2 \rangle / B^2$ [4, 26, 27], which has the form $S^2 \langle p_T^2 \rangle^2$, and is much less dependent on the parameters of the soft model [24, 26, 27] than S^2 on its own. The CEP cross section for Higgs bosons produced by gluon-gluon fusion, and decaying to $b\bar{b}$, is proportional to

$$\frac{\Gamma^{\text{eff}}}{M_H^3} \equiv \frac{\Gamma(H \rightarrow gg)}{M_H^3} \text{BR}(H \rightarrow b\bar{b}) \quad (3)$$

where $\Gamma(H \rightarrow gg)$ is the decay width to gluons and $\text{BR}(H \rightarrow b\bar{b})$ is the branching ratio to $b\bar{b}$ quarks. Comprehensive recent studies performed in [24] show that the effective value of the survival factor (which accounts for the so-called ‘enhanced absorptive corrections’ and other effects violating soft-hard factorization) is

$$\langle S_{\text{eff}}^2 \rangle = 0.015^{+0.01}_{-0.005} \quad (4)$$

for CEP of a SM Higgs of mass around $M = 120$ GeV. Moreover, as discussed in [26], this result should be regarded rather as a conservative (lower) limit for the gap survival. For the SM Higgs width $\Gamma(H \rightarrow gg) = 0.25$ MeV the resulting value for the exclusive cross section is, conservatively,

$$\sigma(pp \rightarrow p + (H \rightarrow b\bar{b}) + p) \simeq 2 \text{ fb}, \quad (5)$$

with an overall uncertainty of a factor of 3 up or down, see also [9, 25]³. The good news is that exclusive dijet [28], $\gamma\gamma$ [29] and χ_c [30] production data from CDF and the leading neutron

³Recall that for central exclusive $b\bar{b}$ production this uncertainty does not affect the physically important signal-to-background ratio, S/B .

data at HERA are in a broad agreement [26, 31, 32] with the basic theoretical formalism of Refs.[4, 21, 22] indicating that it is unlikely that enhanced absorption effects will strongly reduce the exclusive SM Higgs signal at the LHC energy.

3 On the backgrounds to the $p + (H \rightarrow b\bar{b}) + p$ signal

The potential importance of the $p + (H \rightarrow b\bar{b}) + p$ process means that the physical backgrounds to this reaction must be thoroughly addressed. These backgrounds can be broken down into three broad categories: central exclusive, interaction of two soft Pomerons and the so-called overlap background. The last source of background is important when there are a large number of pp interactions in each bunch crossing at the LHC. The largest overlap background is a three-fold coincidence between two soft single diffractive events ($pp \rightarrow pX$), which produce forward protons within the acceptance of the forward detectors, together with an inelastic event, which produces the hard scatter $pp \rightarrow b\bar{b}$ and, thus, can mimic the signal. This important background is the subject of detailed studies [2], and it is shown that, with dedicated fast-timing detectors, and some additional experimental cuts, it can be reduced to a tolerable level, see, for instance [8, 13]. We do not consider this type of background further.

Double-Pomeron-exchange (DPE) is the process $pp \rightarrow p + X + p$, where the central system, X , is produced by an inelastic Pomeron-Pomeron interaction. In this case there are always ‘Pomeron remnants’ accompanying the hard scatter. The DPE $b\bar{b}$ background has been extensively studied in relation to the $H \rightarrow b\bar{b}$ signal, and it has been concluded that this background is negligible after appropriate experimental cuts [8, 15]. We do not consider these types of background events further as well.

Here, our concern is the exclusive $b\bar{b}$ background processes, which are generated by the collisions of the two hard (active) gluons in Fig. 1, labelled x_1, x_2 . The dominant sources of such background were discussed in detail in [5, 6, 14, 16]. It was shown that all these backgrounds are strongly suppressed and controllable and, in principle, can be further reduced by the appropriate optimized cuts on the final state particle configurations in such a way that the signal-to-background ratio, S/B , is of order 1 (or may be even better for MSSM or other BSM schemes [6] - [9], [13]).

The unique advantage of the $p + (H \rightarrow b\bar{b}) + p$ signal is that there exists a $J_z = 0$ selection rule [18, 33], which requires the leading order (LO) $gg^{PP} \rightarrow b\bar{b}$ background subprocess to vanish in the limit of massless quarks and forward outgoing protons. Here the PP superscript is to indicate that each active gluon comes from colour-singlet t -channel (Pomeron) exchange. However, there are still four main sources of gg -generated backgrounds, some of which occur even at LO [6, 14, 17].

- (i) The prolific (LO) $gg^{PP} \rightarrow gg$ subprocess can mimic $b\bar{b}$ production since we may misidentify the gluons as b and \bar{b} jets⁴.

⁴ When calculating the cross section of exclusive gluon-dijet production we neglect the diagrams shown in Fig. 7 and Fig. 8c of [34]. The contribution of the diagram of Fig. 7 is power-suppressed by a factor of Q_t^2/E_T^2 , where E_T is the transverse energy of the jets. For LHC energies, and $M_H = 120$ GeV, the main contribution to

- (ii) An admixture of $|J_z| = 2$ production, arising when the outgoing protons have non-zero p_t , which contributes to the LO $gg^{PP} \rightarrow b\bar{b}$ background.
- (iii) Because of the non-zero mass of the b quark there is a contribution to the $J_z = 0$ $gg^{PP} \rightarrow b\bar{b}$ cross section of order m_b^2/E_T^2 . Here E_T is the transverse energy of the b and \bar{b} jets.
- (iv) There is a possibility of NLO $gg^{PP} \rightarrow b\bar{b}g$ background contributions, which for large angle, hard gluon radiation do not obey the selection rule. In particular, the extra gluon may go unobserved in the direction of a forward proton. This background is reduced by requiring the approximate equality $M_{\text{missing}} = M_{b\bar{b}}$. Calculations [15] show that this background may be safely neglected. The remaining danger is large-angle hard gluon emission, which is collinear with either the b or \bar{b} jet, and, therefore, unobservable. This background source results in a sizeable contribution, see [14], which, together with other pieces listed in items (i-iii), are accounted for in the evaluation [6, 7] of the prospective sensitivities for the exclusive production of scalar Higgs bosons at the LHC.

Among all the QCD backgrounds, the m_b^2/E_T^2 -suppressed dijet $b\bar{b}$ production is especially critical, since it is practically the only irreducible background source, which cannot be decreased, either by improving the hardware (as in the case, when the prolific $gg^{PP} \rightarrow gg$ subprocess mimics $b\bar{b}$ production, with the outgoing gluons misidentified as b and \bar{b} jets [5]) or, for example, by cuts on the three-jet event topology (as in the case of large-angle gluon radiation in the process $gg(J_z = 0) \rightarrow q\bar{q}g$, discussed in [6, 8, 14]). For some time the m_b^2/E_T^2 -suppressed term raised concern, since the result could be strongly affected by large higher-order QCD effects. The good news is, that, as shown in Ref. [16], the one-loop QCD corrections suppress the exclusive $b\bar{b}$ background (by a factor of about 2, or more for larger $b\bar{b}$ -masses), in comparison with that calculated using the Born $gg^{PP} \rightarrow b\bar{b}$ amplitude. This result has been already accounted for in the numerical studies [7] of CEP of MSSM Higgs bosons.

the exclusive amplitude comes from the region of $Q_t \sim 2$ GeV. The small contribution from the $Q_t \sim E_T$ domain can be considered as a minor part of the NLO correction to the LO result. The diagram of Fig. 8c in [34] is treated as part of the Sudakov form factor. However, this diagram does not allow for double logarithms. Even the single-log contribution is questionable here. Recall that, actually, we calculate the *imaginary* part, that is the s -channel discontinuity, of the CEP amplitude. If required the numerically small (for our positive signature case) real part can be restored by including the well known signature factors. The only possible logarithm in the s -channel discontinuity of Fig. 8c is the BFKL-type longitudinal logarithm, which can be removed by choosing the appropriate planar gauge, where the gluon field A_μ is orthogonal to the vector n_μ ($A_\mu n_\mu = 0$), say with $n = (p_1 + p_2)_\parallel$ parallel to the longitudinal part of the dijet momentum $(p_1 + p_2)$. In a different gauge the diagram of Fig. 8c may lead to a longitudinal single-log, coming from the region of relatively low gluon transverse momentum $q_t \ll E_T$. This piece should be summed up, together with other analogous terms caused by permutations of the gluon lines. As discussed in [25] the contribution from the region of very small $q_t < Q_t$ vanishes due to destructive interference between the emission from the active gluon (x) and the screening gluon. To trace this cancellation explicitly we have to consider *all* permutations, which at the single-log accuracy are summed up by the LO BFKL kernel. Using the known BFKL kernel it was shown in [25] (Sect. 5) that the sum of all permutations leads to the effective lower cutoff $q_t = Q_t$ in the integral for the Sudakov-like form factor T . This value of the cutoff provides the single-log accuracy of the T -factor. The NLO contribution of Fig.8c, being not enhanced by any large logarithm, is the part of the NLO corrections, which are beyond the accuracy of our approach.

The $b\bar{b}$ production in the $|J_z| = 2$ state is another sizeable background. In principle, this contribution can be reduced by selecting events with forward outgoing protons of smaller transverse momenta [18]. However, at the moment, among the background sources listed in items(i-iv) above the exclusive gluon-gluon dijet production is one of the most important backgrounds for the CEP Higgs process. In order to suppress further this QCD contribution we need better experimental discrimination between b -quark and gluon jets; that is, to achieve a lower probability $P_{g/b}$ for misidentifying a gluon as a b -jet.

Let us elucidate the physical origin of the suppression of the LO $gg^{PP} \rightarrow b\bar{b}$ subprocess. As discussed in Ref. [14], it is convenient to consider separately the quark helicity conserving (QHC) and the quark helicity non-conserving (QHNC) background amplitudes. As shown in Refs. [14, 35, 36], this suppression is a direct consequence of the symmetry properties of the Born helicity amplitudes, $M_{\lambda_1, \lambda_2}^{\lambda_q, \lambda_{\bar{q}}}$, describing the binary background process

$$g(\lambda_1, p_A) + g(\lambda_2, p_B) \rightarrow q(\lambda_q, p_1) + \bar{q}(\lambda_{\bar{q}}, p_2). \quad (6)$$

Here, the λ_i label the helicities of the incoming gluons, and λ_q and $\lambda_{\bar{q}}$ are the (doubled) helicities of the produced quark and antiquark. The p 's denote the particle four-momenta ($p_A^2 = p_B^2 = 0$, $p_{1,2}^2 = m^2$), with $p_A + p_B = p_1 + p_2$ and $s = (p_A + p_B)^2$. For a colour-singlet, $J_z = 0$, initial state, ($\lambda_1 = \lambda_2 \equiv \lambda$) the Born QHC amplitude with $\lambda_{\bar{q}} = -\lambda_q$ vanishes [36]⁵

$$M_{\lambda, \lambda}^{\lambda_q, -\lambda_q} = 0. \quad (7)$$

For the QHNC amplitude for large-angle production we have

$$M_{\lambda, \lambda}^{\lambda_q, \lambda_q} \sim \mathcal{O}\left(\frac{m_q}{\sqrt{s}}\right) M_{\lambda, -\lambda}^{\lambda_q, -\lambda_q}, \quad (8)$$

where the amplitude on the right-hand-side displays the dominant helicity configuration of the LO background process. The above-mentioned m_b^2 -suppression of the $gg^{PP} \rightarrow b\bar{b}$ Born cross section is a consequence of Eqs. (7) and (8), and, as discussed, it plays a critical role in controlling the $b\bar{b}$ background. However, as was pointed out already in [35], the suppression of the $J_z = 0$ background cross section is removed by the presence of an additional gluon in the final state. The radiative three-jet processes can then mimic the two-jet events in some specific (for instance, quasi-collinear) configurations. Additional gluon radiation from the ‘hard’ subprocess, $gg^{PP} \rightarrow q\bar{q}$, was considered in detail in [14].

Until now, one source of radiative QCD background has not been addressed at the quantitative level. This concerns the contribution from the $b\bar{b}g$ events caused by the ‘internal’ gluon radiation from the spectator screening gluon, see Fig. 2(b). Note that a separation between this ‘internal bremsstrahlung’ and the ‘standard’ gluon radiation from the active gluons and final quarks makes sense only when the momentum p_t of the emitted gluon momenta exceeds

⁵Note that in the massless limit Eq. (7) holds for any colour state of initial gluons. This is a consequence of the general property, that the non-zero massless tree-level amplitudes should contain at least two positive or two negative helicity states, see, for example, [37]. It is a particular case of the more general Maximally-Helicity-Violating amplitude (MHV) rule, see, for example, [38].

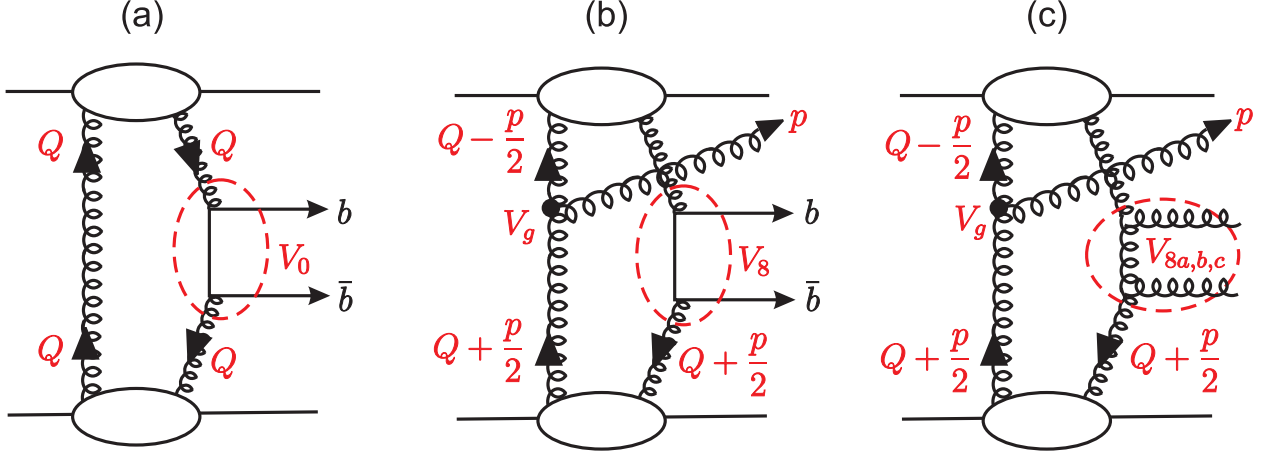


Figure 2: Schematic diagrams for (a) $b\bar{b}$, (b) $b\bar{b} + g$ and (c) $gg + g$ exclusive production, where in (b) and (c) the extra gluon, of 4-momentum p , is radiated from the screening gluon.

the internal transverse momentum in the gluon loop Q_t , since at lower momenta (larger wavelengths) there are interference effects between the different contributions leading to complete cancellation between radiation from the t -channel gluons for $p_t \ll Q_t$.

Potentially this internal bremsstrahlung contribution could be quite sizeable. However, as discussed below, it appears to be numerically small, in particular, because of an additional suppression resulting from symmetry arguments, see [39]. Below, the detailed evaluation of this background source is presented for the first time.

4 Gluon radiation from the screening gluon

First, recall [4] the form of the cross section for non-radiative dijet ($b\bar{b}$) production, that is, for $pp \rightarrow p + b\bar{b} + p$ of Fig. 2(a). Similar to the expression for the Higgs signal, (1), the cross section for the QCD background is given by

$$\sigma(pp \rightarrow p + b\bar{b} + p) \sim \frac{\langle S^2 \rangle}{B^2} \left| \int \frac{dQ_t^2}{Q_t^6} V_0 f_g(x_1, x'_1, Q_t^2, \mu^2) f_g(x_2, x'_2, Q_t^2, \mu^2) \right|^2 \hat{\sigma}(gg^{PP} \rightarrow b\bar{b}), \quad (9)$$

where the expression in front of $\hat{\sigma}$ plays the role of the corresponding gluon-gluon luminosity. In other words, the CEP cross section can be written as

$$\frac{d\sigma^{\text{CEP}}}{dy d\ln M^2} = \frac{dL}{dy d\ln M^2} \cdot \hat{\sigma}, \quad (10)$$

where M and y are the mass and rapidity of the centrally produced system.

The factor V_0 in (9) is the part of the ‘hard’ matrix element arising from the polarization vectors of the active gluons, which depend on their momenta Q . For CEP of dijets, the final system is in a colour-singlet state, and the corresponding factor is just $V_0 = Q_t^2$.

However, we are interested in radiation from the screening gluon, see Fig. 2(b). Now we have two hard matrix elements - the emission of a new gluon in a left part of the diagram and

high E_T dijet production in the right part. Therefore the cross section takes a more complicated form

$$\sigma = L^{\text{eff}} \cdot \hat{\sigma}$$

with

$$\frac{dL^{\text{eff}}}{dy \, d \ln M^2} = \frac{dL}{dy \, d \ln M^2} \frac{N_c \alpha_s(p_t^2)/\pi}{d \ln p_t^2 \, d \eta_3}, \quad (11)$$

where we have already included in (11) the soft bremsstrahlung factor $N_c \alpha_s dp_t^2/\pi p_t^2$. That is, using the BFKL effective gluon vertex, it is still possible to write the cross section in a factorized form with an *effective* luminosity L^{eff} which now depends on the gluon transverse momentum p_t ; η_3 is the rapidity of the bremsstrahlung gluon with momentum p .

There are now four propagators (external to the ‘hard’ matrix element) associated with four gluons with momenta $Q \pm p/2$. Calculating the first factor $dL/dy d \ln M^2$ in (11) we, therefore, have to replace the term $\int dQ_t^2 V_0/Q_t^6$ in (9) by

$$\int \frac{d^2 Q_t}{\pi} \frac{V_g V_8}{(Q - p/2)_t^4 (Q + p/2)_t^4} \quad (12)$$

and, correspondingly, evaluate the unintegrated gluon densities f_g at $q_t = (Q - p/2)_t$ and $q_t = (Q + p/2)_t$. Here p is the momentum of the emitted gluon, while Q_t is the momentum of integration around the gluon loop. For exclusive three-jet ($b\bar{b}g$) production, the high E_T dijet ($b\bar{b}$) system is in a colour-octet state. Thus we have denoted the corresponding polarization factor by V_8 . We shall calculate it explicitly later.

Finally, V_g , in (12), is the vertex factor arising from the emission of the extra gluon. It accounts not only for the diagrams shown in Fig. 2(b,c), but also for soft gluon radiation from the upper and lower blobs as well. The simplest way to calculate V_g is to use the effective vertex of gluon emission in the BFKL approach [40], see also [41]. We choose the frame where the emitted gluon rapidity $\eta_3 = 0$, and direct the axis x along the gluon transverse momentum \vec{p}_t . In this case the gluon polarization has two transverse components, z and y , with vertex factors

$$C_z = 2(Q - p/2)_t \cdot (Q + p/2)_t / |p|, \quad (13)$$

$$C_y = 2Q_y, \quad (14)$$

for the gluons polarized in the z and y directions respectively.

For the CEP of the $b\bar{b}g$ -system we can neglect the term which is linear in Q_t . This term vanishes after angular integration, since the Q_t -component directed along the gluon momentum \vec{p}_t is orthogonal to the gluon polarization vector e_3^μ , while the whole expression is symmetric under the interchange $Q_y \rightarrow -Q_y$. Thus, with the help of the effective BFKL vertex we obtain

$$V_g = (Q - p/2)_t (Q + p/2)_t = (Q_t^2 - p_t^2/4). \quad (15)$$

To calculate the V_8 factor, we can either use the Weizsäcker-Williams method or choose a suitable (planar) gauge. Then, to LO accuracy (both in the collinear, $\ln Q^2$, and BFKL, $\ln(1/x)$, approaches), we can replace the polarization vectors e_i^μ of the t -channel active gluons (of momenta $q_i = Q \pm p/2$) by their transverse momenta. Explicitly, we have $e_i^\mu \simeq q_{it}^\mu/x_i$. The

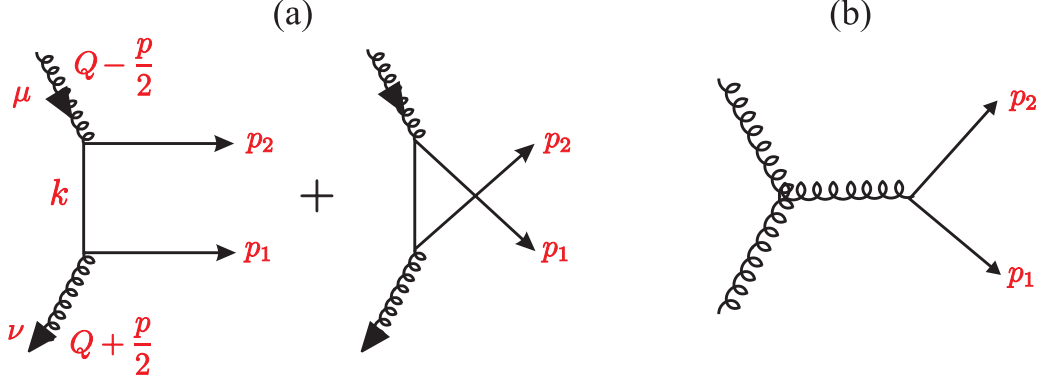


Figure 3: Diagrams for the $gg \rightarrow b\bar{b}$ subprocess.

factor $1/x_i$ is included in the unintegrated gluon densities f_g . As a result, in the calculation of the hard matrix element, we shall write the polarization tensor corresponding to the incoming active gluons, in the form

$$e_1^\mu e_2^\nu \propto T^{\mu\nu} = \left[\left(Q - \frac{p}{2} \right)^\mu \left(Q + \frac{p}{2} \right)^\nu \right]_t. \quad (16)$$

We are now ready to compute the cross sections for, first, the subprocess $gg \rightarrow b\bar{b} + g$, and then for $gg \rightarrow gg + g$, in which a third jet, g , is emitted.

Note that, because of the gluon vertex factors (13,14), the integral (12) for the effective luminosity L^{eff} for gluon bremsstrahlung from the screening gluon is less sensitive to the infrared region than the analogous integral (9) for the standard exclusive luminosity L in the non-radiative case.

5 Exclusive $b\bar{b} + g$ production

First, recall that the x axis is directed along the emitted gluon transverse momentum \vec{p}_t and note, that the component of the tensor $T^{\mu\nu}$ linear in Q_y , that is $Q_y p_x - p_x Q_y$, vanishes for the $gg \rightarrow b\bar{b}$ matrix element in the massless quark limit. Indeed, such a component corresponds to the $J_z = 0$, octet state of the incoming gluons, for which the $gg \rightarrow b\bar{b}$ matrix element vanishes in the massless quark limit, see footnote 5. Therefore, we need consider only the polarization tensor

$$e_1^\mu e_2^\nu \propto T^{\mu\nu} = (Q - p/2)_x (Q + p/2)_x + Q_y Q_y, \quad (17)$$

where the indices xx and yy on the right-hand-side play the role of $\mu\nu$ on the left-hand-side. The contributions to the $gg \rightarrow b\bar{b}$ amplitude, corresponding to Fig. 3(a), contain $\bar{u}(p_1) \not{\epsilon}^\nu \not{k} \not{\epsilon}^\mu v(p_2)$, where k is the t -channel quark momentum. The sum of the contributions with a longitudinal component of k and the contribution of the diagram with s -channel gluon, Fig. 3(b), vanishes in the massless quark limit, analogously to the $J_z = 0$ case. The T^{xx} component gives $\gamma_x \not{q} \gamma_x = \not{q}$ where $\vec{q} = \vec{k}_x - \vec{k}_y$, that is $q_x = k_x$ and $q_y = -k_y$. Similarly, the T^{yy} component gives $-\not{q}$. Thus, when calculating the effective gg luminosity for *octet* $q\bar{q}$ production we have to use

$$V_8 \equiv V_{8q} = \left[\left(Q - \frac{p}{2} \right)_x \left(Q + \frac{p}{2} \right)_x - Q_y Q_y \right], \quad (18)$$

and then to calculate the square of the matrix element, that is $\text{Tr}[\not{q}\not{p}_1\not{q}\not{p}_2]$. The resulting octet $b\bar{b}$ production is

$$\frac{d\hat{\sigma}(b\bar{b})_8}{dt} = \frac{3}{64} \frac{\pi\alpha_s^2(E_T^2)}{M^4} \left(\frac{\cos^2\theta((1 + \cos^2\theta) + \sin^2\theta(1 - 2\cos^2(2\phi)))}{\sin^2\theta} \right). \quad (19)$$

The coefficient $3/64$ accounts for the colour factors, arising both in the $gg \rightarrow b\bar{b}$ subprocess and in the radiation of the additional gluon. In (19), θ is the polar angle of a high E_T jet in the frame where the rapidity of high- E_T dijet system $y_{b\bar{b}} = 0$, and ϕ is the azimuthal angle between the gluon momentum p (i.e. x axis) and the quark jet direction. After integration over this azimuthal angle the second term in the brackets in the numerator of (19) disappears, since $\langle 1 - 2\cos^2(2\phi) \rangle = 0$ in the limit $E_T \gg p_t$.

Instead of working in terms of the dijet variables E_T and $\delta\eta = \eta_1 - \eta_2$ ($\delta\eta$ is the rapidity difference between the two outgoing jets) here, following [4] we use the subprocess variables M^2 and t . It turns out that factors in Jacobian cancel so that we obtain

$$\frac{d\hat{\sigma}}{dt} \bigg/ \frac{dM^2}{M^2} = \frac{d\hat{\sigma}}{dE_T^2} \bigg/ d(\delta\eta).$$

Thus, the product of the luminosity $dL/dy d\ln M^2$ and $d\hat{\sigma}/dt$ gives the differential cross section $d\sigma/dy d(\delta\eta) dE_T^2$.

Note that the integrated cross section vanishes at 90° when $\cos^2\theta = 0$. This is a general property of the QHC $gg \rightarrow b\bar{b}$ amplitudes with $J_z = 2$, see [14, 39]. In order to gain insight into the origin of such a suppression, we note that when $\theta = \pi/2$ in the $b\bar{b}$ rest frame, the final state is asymmetric with respect to a 180° rotation about the quark direction: the overall spin projection onto this direction is ± 1 . At the same time, the initial digluon system is symmetric under this rotation due to the identity of the incoming gluons (protons). This symmetry, in configuration space, is not affected by the colour structure, and, as a result of rotational invariance, the $\theta = \pi/2$ amplitude vanishes [14, 35]. As discussed in Ref.[14], since we are interested in the detection of large angle jets in the central detectors at the LHC, the fact that all $J_z = 2$ QHC cross sections are proportional to $\cos^2\theta$ provides an additional suppression of all such background contributions (by a factor of, at least, ~ 0.2). This suppression provides an improvement of the $b\bar{b}$ signal-to-background.

It is worth mentioning, that, strictly speaking, we have to account for the interference between the radiation from the screening gluon and that from the active gluons and from the final quarks (on the right-hand side of the amplitude in Fig. 2(b)). However, in reality, the amplitude squared, $|A_{\text{scr}}|^2$, corresponding to the emission from the screening gluon is so small that the interference term (which is suppressed as the first power of A_{scr}) is still negligible. Therefore, here we evaluate only the contribution of radiation from the screening gluon and do not consider a more complicated expression for the interference. To illustrate that the amplitude A_{scr} is small we note that for $p_t \ll Q_t$ the polarization tensor $T^{\mu\nu}$ is proportional $(Q^\mu Q^\nu)_t$. Thus after the azimuthal integration, the initial digluon system is in a $J_z = 0$ state. Therefore, the corresponding matrix element for the octet $gg \rightarrow b\bar{b}$ hard subprocess is suppressed by the $J_z = 0$ selection rule. The same is true for emission off the external quarks in the limit $p_t \ll E_T$. This is also suppressed due to the $J_z = 0$ selection rule. At the same time, for relatively large gluon

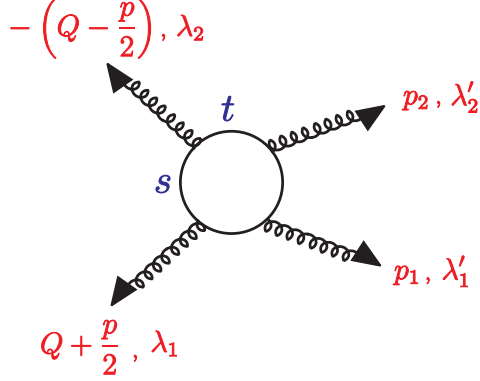


Figure 4: Momenta and helicities of the $gg \rightarrow gg$ subprocess.

momenta, $p_t \gtrsim 2Q_t$, the effective luminosity for exclusive $b\bar{b}g$ production is suppressed by a large factor, $(Q/p)^4$, as compared to the CEP of exclusive dijets. Therefore, we do not need to worry about the explicit calculations of these type of interference.

Moreover, at LHC energies, the typical value of the loop integration momentum is $Q_t \sim 2$ GeV. Now a gluon with $p_t > 2Q_t$, that is a gluon with $p_t \gtrsim 5$ GeV, in a low multiplicity exclusive process should be *observed* experimentally as an individual minijet. Thus such a process should not be considered as a background to exclusive $H \rightarrow b\bar{b}$ production.

6 Exclusive $gg + g$ production

Here we present analytical results for gluon radiation from the screening gluon, which accompanies a hard $gg \rightarrow gg$ process. Recall that exclusive $gg \rightarrow ggg$ production can be a background to exclusive $b\bar{b}$ production, since gluon jets can mimic b jets. To describe the three-gluon exclusive production process of Fig. 2(c) we take the same V_g vertices, (13,14), describing the extra gluon emission, and the same polarization tensor, $T^{\mu\nu}$ of the active gluons, (16), and calculate the corresponding $gg \rightarrow gg$ amplitude of the hard subprocess, where now the two incoming ‘active’ gluons are in a *colour-octet* state.

As in Ref. [14], it is convenient to use the helicity formalism of [38]. The non-zero amplitudes for three basic helicity configurations are

$$\begin{aligned}
 (++; --) &= (--; ++) = C' s^2/tu \\
 (+-; +-) &= (-+; -+) = C' t^2/tu \\
 (+-; -+) &= (-+; +-) = C' u^2/tu,
 \end{aligned} \tag{20}$$

where the notation $(\lambda_1 \lambda_2; \lambda'_1 \lambda'_2) = (++; --)$, etc. corresponds to the helicities of the gluons as defined in Fig. 4. The normalization factor is $C' = 8\pi\alpha_s$, up to a colour coefficient. Here s, t and u are the standard Mandelstam variables for hard $gg \rightarrow gg$ scattering.

In terms of helicity, the elements of the polarization tensor of the active gluons, (16), can be written as

$$(xx + yy)/2 = (++) + (--) \quad (a)$$

$$(xx - yy)/2 = (+-) + (-+) \quad (b)$$

$$i(xy - yx)/2 = (++) - (--) \quad (c)$$

$$i(xy + yx)/2 = (+-) - (-+) \quad (d) \quad (21)$$

Thus, we have to compute the coherent sum of the amplitudes A_{ji} corresponding to the $T^{\mu\nu}$ tensor in initial state for each helicity configuration (ji) in the final state, and then to take the sum $\sum_{ji} |A_{ji}|^2$. Recall that the initial states $(++)$, $(--)$, $(+-)$, $(-+)$ correspond to the di-gluon J_z projection equal to 0, 0, +2 and -2 respectively. Obviously, these states do not interfere with each other.

Again we neglect the interference with amplitudes where the third gluon is radiated from the hard subprocess. Therefore, we have to calculate the effective luminosities⁶, which contain the soft bremsstrahlung factor for the extra gluon. L^a , L^b , L^c for the initial polarization states (a, b, c) . Note that for (d) the corresponding luminosity, L^d , is very small: in terms of the $T^{\mu\nu}$ tensor, (16), L^d results from the $Q_x Q_y + Q_y Q_x$ component, which vanishes due to $Q_x \leftrightarrow -Q_x$ symmetry⁷.

The effective luminosities $L^a(0)$, $L^b(2)$, which correspond to $J_z = 0, 2$, can be calculated using the vertex factor V_g of (15), and using the combinations which give the appropriate V_8 factors

$$V_{8a} = (Q^2 - p^2/8) \quad \text{and} \quad V_{8b} = -p^2/8. \quad (22)$$

Similarly, the luminosity $L^c(0)$, which corresponds to $J_z = 0$, can be obtained using the vertex factor $V_g = Q_y$ and

$$V_{8c} = |Q| |p|. \quad (23)$$

Finally, these luminosities should be multiplied by the corresponding $J_z = 0, 2$ cross sections for s -channel *octet* $gg \rightarrow gg$ hard scattering. We find

$$\frac{d\sigma^{(0)}}{dt} = C \frac{\pi\alpha_s^2}{E_T^4} \quad (24)$$

and

$$\frac{d\sigma^{(2)}}{dt} = C \frac{\pi\alpha_s^2}{E_T^4} \cos^2\theta, \quad (25)$$

where the coefficient $C = 9/16$ incorporates all colour factors.

7 Numerical results and discussion

For illustration, we consider the exclusive production of a central system of mass $M = 120$ GeV at rapidity $y = 0$ and LHC energy $\sqrt{s} = 14$ TeV. The effective luminosities⁸, L^{eff} of (11), of exclusive processes with radiation from the screening gluon are shown in Fig. 5.

⁶The effective luminosities are defined in eq. (11).

⁷This symmetry could be violated by a different scale q_t^2 behaviour of the unintegrated gluons $f_g(x_i, x'_i, q_t^2, \mu^2)$ at different values of x_1 and x_2 , but this effect is negligibly small.

⁸Note, that the soft gap survival factor S^2 is not included in the luminosities, L^{eff} , which are shown in Fig. 5.

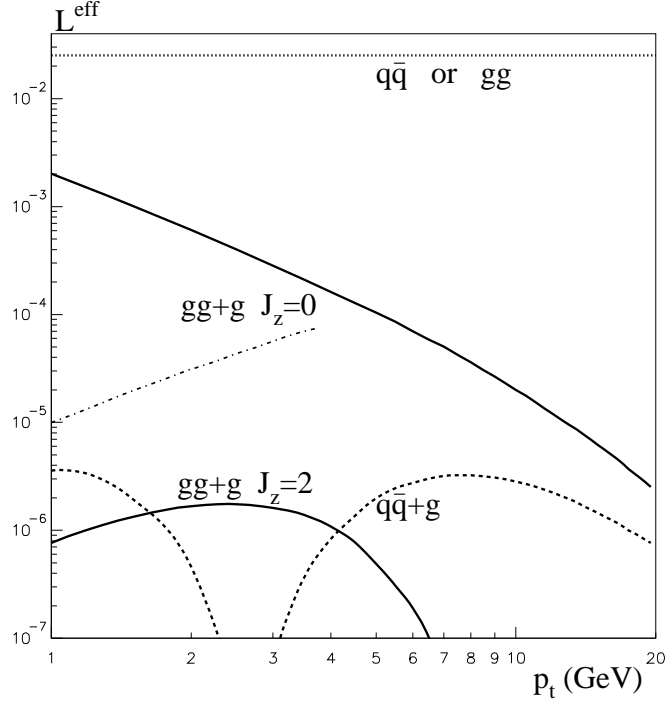


Figure 5: The effective luminosities, L^{eff} of (11), versus transverse momentum, p_t of the bremsstrahlung gluon, for the colour-octet radiative processes ($pp \rightarrow p + q\bar{q}g + p$ and $pp \rightarrow p + ggg + p$) for $\sqrt{s} = 14$ TeV, $y = 0$ and $M = 120$ GeV. The curves are for the case of $\eta_3 = 0$, however, as far as the bremsstrahlung gluon energy does not drastically affect the overall kinematics the results are independent on η_3 . In this plot we use the notation $q\bar{q}$, as it is sufficient to treat the b quark here as massless.

7.1 Results for exclusive $b\bar{b} + g$ production

First, we consider the effect of gluon radiation (from the screening gluon) which accompanies exclusive $b\bar{b}$ production, as shown in Fig. 2(b). Recall that exclusive QCD $b\bar{b}$ production is the main irreducible background to CEP of a Higgs boson which decays via the $H \rightarrow b\bar{b}$ mode. In the absence of gluon radiation, the $J_z = 0$ selection rule [18], suppresses the QCD production of the quark-antiquark pair by a factor of m_b^2/M^2 . Since the radiation of an additional gluon does not obey the selection rule, the $b\bar{b} + g$ background (which is not suppressed by the m_b^2/M^2 ratio⁹) could potentially become comparable with the original LO background. However, this is not the case. In Fig. 5 the dotted line, marked $q\bar{q}$ (or gg), shows the luminosity which is to be convoluted with the LO binary $gg \rightarrow b\bar{b}$ (or $gg \rightarrow gg$) colour singlet cross section. On the other hand, the effect of radiation of an extra gluon from the screening t -channel gluon is evaluated as the product of L^{eff} (shown by the dashed line marked $b\bar{b} + g$)¹⁰ by the octet cross

⁹Since we are looking for the contribution which is not suppressed by the small m_b^2/M^2 factor, it is sufficient to calculate the corresponding cross section treating the b quark as massless.

¹⁰Note, that the origin of the dip in the region $p_t \sim 2.5$ GeV is just a consequence of gauge invariance, which leads to the factor $(Q - p/2)_t(Q + p/2)_t$ in equations (15,16).

section (19). We see that this luminosity (dashed line) is about four orders of magnitude lower than that for binary $b\bar{b}$ exclusive production (dotted line)¹¹.

Note that the cross section of the hard-octet subprocess (19) vanishes at 90° . After the integration over an appropriate angular interval, $60^\circ < \theta < 120^\circ$, we find that the ratio of the octet $b\bar{b}$ and the LO singlet $b\bar{b}$ subprocess cross sections is

$$\frac{\hat{\sigma}(b\bar{b})_8}{\hat{\sigma}(b\bar{b})_0} = 4.7. \quad (26)$$

Recall that the LO cross section, $\hat{\sigma}(b\bar{b})_0$, is suppressed by a factor of m_b^2/E_T^2 . The NLO correction to $\hat{\sigma}(b\bar{b})_0$ [16] reduces the cross section by a further factor of about 2, and so increases the ratio (26) by this factor. However, when we account for the huge difference of the corresponding luminosities we see that, despite the large ratio $\hat{\sigma}(b\bar{b})_8/\hat{\sigma}(b\bar{b})_0$, the background caused by radiation from the screening gluon is negligible in comparison with the irreducible background due to exclusive $b\bar{b}$ production.

Up to now we discuss just the case when the relatively soft gluon in exclusive $b\bar{b} + g$ production is emitted from the screening (left in Fig.2) gluon. Since the corresponding amplitude is very small a larger contribution may come from the interference between the gluon emission from the hard matrix element and the screening gluon. On the other hand, as we have seen, the probability of the octet $b\bar{b}$ pair production accompanied by the emission from the screening gluon is more than a factor $|F|^2 \sim 10^{-4}$ (four orders of magnitude) smaller than the probability of exclusive singlet $b\bar{b}$ production. The corresponding interference contribution should be suppressed at least by $F \sim 10^{-2}$ and thus will be also negligible in comparison with the irreducible $b\bar{b}$ background.

7.2 Results for exclusive $gg + g$ production

Now we turn to exclusive digluon production. The two continuous curves in Fig. 5 show the effective luminosities for gluon dijet production accompanied by an extra gluon radiated from the screening gluon, see Fig. 2(c). The difference in these luminosities reflects the difference in the quantum numbers of the active incoming di-gluon system. The upper curve corresponds to $J_z = 0$, while the lower ($J_z = 2$) curve is suppressed by s -channel helicity conservation [18]; in the limit of $p_t \rightarrow 0$ we return to the $J_z = 0$ selection rule. It is worth mentioning that the difference between the ‘ $gg + g$ ’ and the ‘ $q\bar{q} + g$ ’ effective luminosities, which both correspond to $J_z = 2$, follows from the fact that the large-angle $gg \rightarrow b\bar{b}$ QHC amplitude in the massless limit should be P -even, and thus, the contribution generated by the term (14) vanishes.

¹¹As mentioned in Section 4, the expression for the effective luminosity L^{eff} is less sensitive to the infrared region than the analogous result for the standard exclusive luminosity L corresponding to the non-radiative case. To quantify the role of the contribution coming from low values of $(Q_t \pm p_t/2)$, we calculate the value of L^{eff} using different infrared cutoffs. At $p_t = 6$ GeV the cutoff of $Q_t \pm p_t/2 > 1$ GeV decreases the amplitude of exclusive $b\bar{b} + g$ production (with gluon emission from the screening gluon) by about 20 %. On the other hand, since the factor V_{8q} in (18) can change sign, in the dip region ($p_t = 2 - 3$ GeV) the amplitude becomes even larger than without the cutoff (but is still small). In any case, the contribution coming from the infrared region is beyond the perturbative QCD framework. Therefore, when calculating the curves in Fig. 5 we introduce our standard infrared cutoff of 0.85 GeV.

When evaluating the physical $b\bar{b}$ background contribution caused by the $gg + g$ events, the corresponding $gg \rightarrow gg$ cross section should be multiplied by a very small factor, $P_{g/b}^2$, see [5]; where $P_{g/b} \sim 0.01$ is the probability of misidentification of a gluon jet as a b -quark jet. As a result, this background contribution also becomes numerically negligibly small as compared to the main irreducible background, $gg^{PP} \rightarrow b\bar{b}$.

Finally, we note that, at first sight, the $J_z = 0$ contribution at very low p_t is quite large. The corresponding effective luminosity, shown by a solid line, is only an order of magnitude lower than that for two-gluon CEP production. However, as already discussed, at such low p_t , it is necessary to include the destructive interference with soft-gluon emission in the matrix element of the hard subprocess. Accounting for these interference effects, we arrive at the final result shown by the dot-dashed curve in Fig. 5. To calculate the amplitude of soft-gluon emission (within the $d \ln p_t^2 d\eta_3$ element of phase space in the beam direction) from the ‘hard’ matrix element, we have to multiply the known amplitude of exclusive gluon dijet production [4] by the soft bremsstrahlung factor $\sqrt{N_c \alpha_s(p_t^2)/\pi}$ ¹².

8 Summary

One of the advantages of exclusive processes is that the major irreducible QCD $b\bar{b}$ background is strongly suppressed by a $J_z = 0$ selection rule, which leads to a factor m_b^2/E_T^2 in the CEP cross section. This offers the unique possibility to observe an exclusive Higgs boson in its main decay mode, $H \rightarrow b\bar{b}$. However, the suppression can be removed by the presence of an additional gluon in the final state. The radiation from the matrix element of a ‘hard’ subprocess was considered in [14]. Here, we have explicitly calculated the effect of radiation from the screening gluon for the case of $b\bar{b} + g$ and $gg + g$ final states, where the $b\bar{b}$ or gg dijets are in a colour-octet state. (The $gg + g$ configuration was studied to allow for the possibility that gluon jets may be misidentified as b -quark jets.) We found that these channels give a completely negligible contribution to QCD background to exclusive $pp \rightarrow p + (H \rightarrow b\bar{b}) + p$ production at the LHC; much less than the already suppressed exclusive $b\bar{b}$ production, $pp \rightarrow p + (b\bar{b}) + p$.

Acknowledgements

We thank Albert De Roeck, Risto Orava, Andy Pilkington, Marek Tasevsky and James Stirling for useful discussions. MGR thanks the IPPP at the University of Durham for hospitality. The work was supported by grant RFBR 07-02-00023, by the Russian State grant RSGSS-3628.2008.2.

¹²We do not continue the dot-dashed curve into the domain of larger p_t since: i) a gluon with larger p_t can be observed experimentally as a separate jet, ii) for larger p_t a more precise and complicated expression for the radiation from the hard matrix element should be used.

References

- [1] G. Weiglein *et al.*, (LHC/LC Study Group Collaboration), [arXiv:hep-ph/0410364](#); S. Heinemeyer, Acta Phys. Polon. B **39**, 2673 (2008) [[arXiv:0807.2514 \[hep-ph\]](#)]; A. Djouadi and R.M. Godbole, [arXiv:0901.2030 \[hep-ph\]](#), and references therein.
- [2] M.G. Albrow *et al.*, [FP420 R&D Collaboration], [arXiv:0806.0302 \[hep-ex\]](#).
- [3] P.J. Bussey, [arXiv:0809.1335 \[hep-ex\]](#); M. Grothe [CMS Collaboration], [arXiv:0806.2977 \[hep-ex\]](#); D. d’Enterria, [arXiv:0905.4307 \[hep-ex\]](#).
- [4] V.A. Khoze, A.D. Martin, M.G. Ryskin, Eur. Phys. J. C **23**, 311 (2002).
- [5] A. De Roeck *et al.* Eur. Phys. J. C **25**, 391 (2002).
- [6] S. Heinemeyer *et al.*, Eur. Phys. J. C **53**, 231 (2008) [[arXiv:0708.3052 \[hep-ph\]](#)].
- [7] S. Heinemeyer *et al.* [arXiv:0811.4571 \[hep-ph\]](#).
- [8] B.E. Cox, F.K. Loebinger and A.D. Pilkington, JHEP **0710**, 090 (2007) [[arXiv:0709.3035 \[hep-ph\]](#)].
- [9] A. Kaidalov *et al.*, Eur. Phys. J. C **33**, 261 (2004), [hep-ph/0311023](#).
- [10] J.R. Ellis, J.S. Lee and A. Pilaftsis, Phys. Rev. D **71**, 075007 (2005) [[arXiv:hep-ph/0502251](#)].
- [11] J.R. Forshaw *et al.*, JHEP **0804**, 090 (2008) [[arXiv:0712.3510 \[hep-ph\]](#)].
- [12] C. Royon, Acta Phys. Polon. B **39**, 2339 (2008) [[arXiv:0805.0261 \[hep-ph\]](#)].
- [13] M. Chaichian *et al.*, [arXiv:0901.3746 \[hep-ph\]](#), JHEP in press.
- [14] V.A. Khoze, M.G. Ryskin and W.J. Stirling, Eur. Phys. J. C **48**, 477 (2006) [[arXiv:hep-ph/0607134](#)].
- [15] V.A. Khoze, A.D. Martin and M.G. Ryskin, Phys. Lett. B **650**, 41 (2007) [[arXiv:hep-ph/0702213](#)].
- [16] A.G. Shuvaev, V.A. Khoze, A.D. Martin and M.G. Ryskin, Eur. Phys. J. C **56**, 467 (2008) [[arXiv:0806.1447 \[hep-ph\]](#)].
- [17] V.A. Khoze, M.G. Ryskin and A.D. Martin, in ‘*Hamburg 2007, Blois07, Forward physics and QCD*’, p.452-458.
- [18] V.A. Khoze, A.D. Martin and M.G. Ryskin, Eur. Phys. J. C **19**, 477 (2001) [Erratum-ibid. C **20**, 599 (2001)] [[arXiv:hep-ph/0011393](#)].
- [19] A.B. Kaidalov *et al.*, Eur. Phys. J. C **31**, 387 (2003) [[arXiv:hep-ph/0307064](#)].

- [20] V.A. Khoze, A.D. Martin and M.G. Ryskin, Eur. Phys. J. C **34**, 327 (2004).
- [21] V.A. Khoze, A.D. Martin, M.G. Ryskin, Eur. Phys. J. C **14**, 525 (2000) [arXiv:hep-ph/0002072].
- [22] V.A. Khoze, A.D. Martin and M.G. Ryskin, Eur. Phys. J. C **18**, 167 (2000) [arXiv:hep-ph/0007359].
- [23] M.G. Ryskin, A.D. Martin and V.A. Khoze, Eur. Phys. J. C **54**, 199 (2008); E.G.S. Luna *et al.*, Eur. Phys. J. C **59**, 1 (2009), arXiv:0807.4115 [hep-ph].
- [24] M.G. Ryskin, A.D. Martin and V.A. Khoze, Eur. Phys. J. C **60**, 265 (2009) [arXiv:0812.2413 [hep-ph]].
- [25] V.A. Khoze, A.D. Martin and M.G. Ryskin, Eur. Phys. J. C **55**, 363 (2008) [arXiv:0802.0177 [hep-ph]].
- [26] A.D. Martin, M.G. Ryskin and V.A. Khoze, Acta Phys. Pol. B **40**, 1841 (2009) [arXiv:0903.2980 [hep-ph]].
- [27] V.A. Khoze, A.D. Martin, M.G. Ryskin and W.J. Stirling, Eur. Phys. J. C **35**, 211 (2004) [arXiv:hep-ph/0403218].
- [28] T. Aaltonen *et al.* [CDF Collaboration], Phys. Rev. **D77**, 052004 (2008).
- [29] T. Aaltonen *et al.* [CDF Collaboration], Phys. Rev. Lett. **99**, 242002 (2007).
- [30] T. Aaltonen *et al.* [CDF Collaboration], Phys. Rev. Lett. **102**, 242001 (2009).
- [31] A.B. Kaidalov, V.A. Khoze, A.D. Martin and M.G. Ryskin, Eur. Phys. J. C **47**, 385 (2006) [arXiv:hep-ph/0602215]; V.A. Khoze, A.D. Martin and M.G. Ryskin, JHEP **0605**, 036 (2006).
- [32] V.A. Khoze, A.D. Martin and M.G. Ryskin, Frascati Phys. Ser. **44**, 147 (2007) [arXiv:0705.2314].
- [33] V.A. Khoze, A.D. Martin and M.G. Ryskin, arXiv:hep-ph/0006005, *in* Proc. of 8th Int. Workshop on Deep Inelastic Scattering and QCD (DIS2000), Liverpool, ed. by J.Gracey, T.Greenshaw (World Scientific, 2001), p.592.
- [34] J.R. Cudell, A. Dechambre, O.F. Hernandez and I.P. Ivanov, Eur. Phys. J. C **61**, 369 (2009) [arXiv:0807.0600].
- [35] D.L. Borden, V.A. Khoze, W.J. Stirling and J. Ohnemus, Phys. Rev. **D50**, 4499 (1994).
- [36] V.S. Fadin, V.A. Khoze and A.D. Martin, Phys. Rev. **D56** (1997) 484.
- [37] S.J. Parke and T.R. Taylor, Phys. Rev. Lett. **56** (1986) 2459; F.A. Berends and W.T. Giele, Nucl. Phys. **B306** (1988) 759.

- [38] M.L. Mangano and S.J. Parke, Phys. Rept. **200**, 301 (1991).
- [39] V.A. Khoze, A.D. Martin and M.G. Ryskin, Eur. Phys. J. C **26**, 229 (2002) [arXiv:hep-ph/0207313].
- [40] E.N. Antonov, L.N. Lipatov, E.A. Kuraev and I.O. Cherednikov, Nucl. Phys. B **721**, 111 (2005) [arXiv:hep-ph/0411185].
- [41] V.S. Fadin, E.A. Kuraev, and L.N. Lipatov, Phys. Lett. B **60**, 50 (1975);
 E.A. Kuraev, L.N. Lipatov, and V.S. Fadin, Zh. Eksp. Teor. Fiz. **71**, 840 (1976) [Sov. Phys. JETP **44**, 443 (1976)]; *ibid.* **72**, 377 (1977) [**45**, 199 (1977)];
 I.I. Balitsky and L.N. Lipatov, Yad. Fiz. **28**, 1597 (1978) [Sov. J. Nucl. Phys. **28**, 822 (1978)];
 L. N. Lipatov, Phys. Rept. **286**, 131 (1997) [arXiv:hep-ph/9610276].